Published in final edited form as:

Endocr Relat Cancer. 2016 September ; 23(9): 747–758. doi:10.1530/ERC-16-0142.

EMT Reversal in human cancer cells after IR knockdown in hyperinsulinemic mice

Zara Zelenko[1], **Emily Jane Gallagher**[1], **Irini Markella Antoniou**[1], **Deepali Sachdev**[2], **Anupma Nayak**[3], **Douglas Yee**[2], and **Derek LeRoith**[1]

[1]Division of Endocrinology, Diabetes and Bone Diseases, Icahn School of Medicine at Mount Sinai, One Gustave L. Levy Place, Box 1055, New York, NY, USA

[2]Department of Medicine and Masonic Cancer Center, University of Minnesota, 424 SE Harvard St, Minneapolis, MN 55455

[3]Department of Pathology and Laboratory Medicine, The Mount Sinai Hospital and Icahn School of Medicine at Mount Sinai, 1468 Madison Ave, New York, NY, USA.

Abstract

Type 2 Diabetes (T2D) is associated with increased cancer risk and cancer-related mortality. Data herein show that we generated an immunodeficient hyperinsulinemic mouse by crossing the $Rag1^{-/-}$ mice, which have no mature B or T lymphocytes, with the MKR mouse model of T2D to generate the $Rag1^{-/-}$ (Rag/WT) and $Rag1^{-/-}/MKR^{+/+}$ (Rag/MKR) mice. The female Rag/MKR mice are insulin resistant and have significantly higher non-fasting plasma insulin levels compared to the Rag/WT controls. Therefore, we used these Rag/MKR mice to investigate the role of endogenous hyperinsulinemia on human cancer progression. In this study we show that hyperinsulinemia in the Rag/MKR mice increases the expression of mesenchymal transcription factors, *TWIST1* and *ZEB1*, and increases the expression of the angiogenesis marker, vascular endothelial growth factor A (*VEGFA*). We also show that silencing the insulin receptor (IR) in the human LCC6 cancer cells leads to decreased tumor growth and metastases, suppression of mesenchymal markers Vimentin, SLUG, TWIST1, and ZEB1, suppression of angiogenesis markers, VEGFA and VEGFD, and re-expression of the epithelial marker, E-cadherin. The data in this paper demonstrate that IR knockdown in primary tumors partially reverses the growth promoting effects of hyperinsulinemia as well as highlighting the importance of the insulin receptor signaling pathway in cancer progression, and more specifically in epithelial-mesenchymal transition.

Keywords

Type 2 Diabetes; Cancer; Hyperinsulinemia; Insulin Receptor; Epithelial-Mesenchymal Transition

Corresponding Author: Derek LeRoith, Division of Endocrinology, Diabetes and Bone Diseases, Icahn School of Medicine at Mount Sinai, One Gustave L. Levy Place, Box 1055, New York, NY 10029, Tel: 212-241-6306, Fax: 212-241-4159, Derek.LeRoith@mssm.edu.

Declaration of Interest

The authors disclose no potential conflicts of interest.

Introduction

Both obesity and Type 2 diabetes (T2D) are associated with increased cancer risk and cancer-related mortality (Haslam and James 2005; Onitilo, et al. 2012; Zhang, et al. 2012). Obesity and T2D may contribute to cancer development and progression through several potential mechanisms. Both metabolic disorders are associated with systemic insulin resistance, hyperinsulinemia and increased growth factors, such as insulin-like growth factor 1 (IGF1), and altered adipokines, including adiponectin and leptin, that are reported to promote tumor growth and progression (Hursting, et al. 2012). Furthermore, systemic and local adipose tissue inflammation with macrophage inflammation is prevalent in obesity and has been shown to contribute to tumor progression (Howe, et al. 2013; Morris, et al. 2013). Dyslipidemia is also a clinical characteristic of obesity and T2D and has been shown to contribute to breast cancer progression in mouse models (Alikhani, et al. 2013).

Of all the possible factors involved in cancer progression and mortality, hyperinsulinemia is apparently the most egregious. A strong association between circulating insulin and lower progression-free survival has been shown in multiple studies (Eliassen, et al. 2007; Goodwin, et al. 2002).

To study whether endogenous hyperinsulinemia promotes the growth and progression of human metastatic cancer, we generated an immune deficient MKR mouse by crossing the Recombination Activating Gene 1 deleted ($Rag1^{-/-}$) mouse with the hyperinsulinemic MKR mouse. The $Rag1^{-/-}$ has been characterized as B and T cell deficient whereas innate immunity is still functional (Mombaerts, et al. 1992). The lack of B and T cell allowed us to introduce human cancer cells to test the effect of hyperinsulinemia on tumor growth and metastases. In this study we characterized the novel $Rag1^{-/-}/MKR^{+/+}$ (Rag/MKR) mice, an immunodeficient T2D mouse model. We induced human metastatic cancer cells (LCC6, a metastatic variant of the MDA-MB-435 cells) in the Rag/MKR and Rag/WT control mice. The origin of the MDA-MB-435 cells is controversial and it has been noted that the MDA-MB-435 cells display characteristics of both breast cancer and melanoma (Chambers 2009). Although the origin is controversial, we used the variant of the MDA-MB-435 cells because they are an established metastatic human cancer cell line, with expression of both epithelial and melanocyte markers (Chambers 2009). Our results determined that endogenous hyperinsulinemia profoundly increased the growth of human LCC6 cancers and that insulin receptor knockdown led to significantly decreased tumor growth in control and hyperinsulinemic mice. Furthermore, the knockdown of the insulin receptor led to changes in tumor signaling and uncovered the down-regulation of mesenchymal markers and re-expression of epithelial marker, E-cadherin. To our knowledge this is the first study to show that hyperinsulinemia promotes the increase in epithelial-mesenchymal transition (EMT) gene expression in human tumor xenografts. Moreover, this is the first study to show that insulin receptor knockdown leads to a reversal of the epithelial-mesenchymal phenotype in any human tumor xenografts.

Methods

Animal models

The hyperinsulinemic female MKR mouse has been well characterized and described in previous publications (Ferguson, et al. 2012; Fernandez, et al. 2001; Novosyadlyy, et al. 2010). Briefly the male mouse develops T2D with insulin resistance, hyperinsulinemia, hyperglycemia and hyperlipidemia between 7–8 weeks of postnatal life, and is non-obese since the model was developed by genetically engineering severe muscle insulin resistance. The female mouse, on the other hand, is insulin resistant and hyperinsulinemic, but has normal blood glucose and lipid levels, and thus is a model of endogenous hyperinsulinemia in the absence of obesity and overt diabetes.

The $Rag1^{-/-}$ mice on a Friend Virus B (FVB) background, a kind gift of Dr. Lisa Coussens (Oregon Health and Science University, Portland Oregon), were crossed with the $MKR^{+/+}$ mouse to generate homozygous $Rag1^{-/-}/MKR^{+/+}$ (Rag/MKR) mice. All mice used in these studies were backcrossed to an FVB/National Institutes of Health (FVB/n) background. Tumor studies were commenced in female mice between 8 and 10 weeks of age.

Animal Studies

All mouse procedures were in compliance with the current standards specified in the Guide of the Care and Use of Laboratory Animals provided by the Association for Assessment and Accreditation of Laboratory Animal Care (AAALAC) and approved by Mount Sinai Institutional Animal Care and Use Committee. The mice were housed 4–5 per cage, kept on a 12-hour light/dark cycle and fed a regular chow diet (PicoLab 5053, Brentwood, MO, USA). At 8 weeks of age, 5×10^6 LCC6 control or LCC6 insulin receptor knockdown cells, resuspended in 100ul of DMEM were injected into the 4^{th} mammary fat pad of Rag/WT and Rag/MKR mice, 8–10 mice per group. For all studies, body weight was monitored weekly, and tumor size was measured twice weekly with calipers. The formula used for the calculating tumor volume was: Volume = 4/3 × pi × (length/2 × width/2 × depth/2). In order to analyze the pulmonary metastasis, post mortem lungs were inflated with 10% formalin, paraffin embedded, sectioned and hematoxylin and eosin stained. Micro-metastasis were examined under the microscope by a pathologist (Dr. A. Nayak).

Real Time qPCR

RNA was extracted from cells using the RNeasy Mini Kit (QIAGEN, Valencia, CA, USA) according to the manufacturer's instructions. One ug of RNA was reverse-transcribed to cDNA using oligo (dT) primers with a RT-PCR kit according to the manufacturer's instructions (Invitrogen, Carlsbad, CA). Following reverse transcription, cDNA was subjected to real time-PCR using the QuantiTect SYBR green PCR kit (QIAGEN, Valencia, CA) in ABI PRISM 7900HT sequence detection systems (Applied Biosystems, Foster City, CA). Insulin Receptor Primers: 5’TACCCCGGAGAGGTGTGTC; 3’CCCGGAAGAGCAGCAAGTAA. ZEB1 primers: 5’CAGAGGATGACCTGCCAACA; 3’GCCCTTCCTTTCCTGTGTCAT. SLUG primers: 5’TTTCTGGGCTGGCCAAACAT; 3’TTCTCCCCCGTGTGAGTTCTA. TWIST1 primers: 5’GCCGGAGACCTAGATGTCATT; 3’CCCACGCCCTGTTTCTTTGA. VEGFA primers:

5’AGGCCAGCACATAGGAGAGA; 3’TTTCTTGCGCTTTCGTTTTT. VEGFD primers: 5’CCATCCAGATCCCTGAAGAA; 3’TTCCAGCAAGTGGATTTTCC. Ribosomal protein L19 (RPL19) housekeeping gene primers: 5’AGCTCTTTCCTTTCGCTGCT; 3’GATCTGCTGACGGGAGTTGG.

Cell Culture

The LCC6 parental, LCC6 control (Ctrl) and LCC6 insulin receptor knockdown (IRKD) clone IR6 cells are previously described (Zhang, et al. 2010). Cells were grown in Dulbecco’s Modified Eagles Medium (DMEM) supplemented with 10% Fetal Bovine Serum (FBS) (Invitrogen Life Technologies, Grand Island, NY), 100U/ml penicillin and 100ug/ml streptomycin (Mediatech, Manassas, VA). Cells transfected with shRNA were maintained in medium supplemented with 1.5ug/ml puromycin. All cells were grown at 37C in 5% CO2 atmosphere.

Western Blotting

LCC6 Ctrl and LCC6 IRKD cells and tumor tissue were lysed in ice-cold lysis buffer containing 50 mM Tris, 150 mM NaCl, 1 mM EDTA, 1.25% CHAPS, 1 mM sodium orthovanadate, 10 mM sodium pyrophosphate, 8 mM B-glycerophosphate and Complete Protease Inhibitor Cocktail tablet (Roche, Indianapolis, IN). The protein concentration of the cells and tumors was measured using the BCA protein assay kit (Thermo Scientific, Rockford, IL). 25ug of protein sample was resuspended in 3× loading buffer supplemented with DTT (Cell Signaling Technologies, Danvers, MA). The samples were denatured at 96°C for 5min. The prepared samples were run on SDS-PAGE 8–16% Tris-glycine gel (Invitrogen Life Technologies, Grand Island, NY) and transferred to nitrocellulose membrane. After overnight incubation at 4°C with primary antibodies, the membranes were incubated with secondary antibodies (Li-Cor Biosciences, Lincoln, NE) and scanned using the Li-Cor infrared imaging system. The western bands were quantified using open source Image J software (National Institutes of Health, Bethesda, MD).

Antibodies

The Western Blot nitrocellulose membranes were probed with the following primary antibodies: anti-phospho–IGF1 Receptor $B^{(Tyr1150/1151)}$/-phospho IR $B^{(Tyr1135/1136)}$, anti-c-MYC, anti-ZEB1, anti-SLUG, anti-Vimentin, anti-phospho $AKT^{(Ser473)}$, anti-total AKT, anti-phospho p44/42 mitogen-activated protein kinase (ERK1/2) $^{(Thr202/Tyr204)}$, anti-total p44/42 mitogen-activated protein kinase (ERK1/2), anti-phospho S6 Ribosomal $Protein^{(Ser235/236)}$, anti-total S6 Ribosomal Protein, (Cell Signaling Technology, Danvers, MA), anti-IR, anti-IGF1R, anti-TWIST1 (Santa Cruz Biotechnology, Dallas, TX), and B-actin (Sigma-Aldrich, St. Louis, MO).

Metabolic Studies

Body weight was measured once a week from 3-weeks to 10-weeks of age. Plasma in non-fasting state was collected in heparinized capillary tubes for insulin quantification. Plasma insulin levels were measured by using the Ultra Sensitive Mouse Insulin ELISA kit according to manufacturer’s instructions (Crystal Chem, Downers Grove, IL). Serum

adiponectin and serum leptin levels were measured by using the Ultra Sensitive Mouse Adiponectin and Ultra Sensitive Leptin ELISA kits respectively according to manufacturer's instructions (Crystal Chem, Downers Grove, IL). Body composition was determined in non-anesthetized mice using the EchoMRI 3-in-1 NMR system (Echo Medical Systems, Houston, TX). Insulin tolerance test was performed on 8-week old mice fasted for 2 hours. Insulin (0.75 units/kg) was injected intraperitoneally. Blood glucose levels were measured immediately before injection at time 0 and at 15, 30, and 60 minutes after insulin injection using Bayer Contour Next Glucometer (Bayer HealthCare, Mishawaka, IN). Weekly blood glucose measurements on non-fasted animals were taken using Bayer Contour Next Glucometer (Bayer HealthCare, Mishawaka, IN). Glucose tolerance test was performed on 8-week old mice fasted for 8 hours. Glucose (2g/kg) was injected intraperitoneally. Blood glucose levels were measured immediately before glucose injection at time 0 and at 15, 30, 60 and 120 minutes using Bayer Contour Next Glucometer. Serum triglyceride and serum cholesterol levels were performed using the Pointe Scientific Liquid Triglyceride and Liquid Cholesterol kits respectively per the manufacturer's instructions (Pointe Scientific, Canton, MI).

Statistical analysis

All data are expressed as mean ± SEM. Student's t-test and, where appropriate, two-way ANOVA followed by Tukey HSD post-hoc test, was used with P value ≤ 0.05 considered statistically significant using GraphPad Prism Software (La Jolla, CA).

Results

Metabolic Phenotype of the Rag/MKR mice

As the immune system may play a role in the development of insulin resistance (DeFuria, et al. 2013), we characterized the metabolic phenotype of the $Rag1^{-/-}/MKR^{+/+}$ (Rag/MKR) mice and $Rag1^{-/-}$ (Rag/WT) controls, in both male and female mice. Body weights were measured weekly. Male and female Rag/MKR mice demonstrated lower body weight, of approximately 3–4g, compared to age and gender matched Rag/WT control mice throughout the from 3–10 weeks of age (Figure 1A). In addition, they showed less whole body fat compared to Rag/WT controls at 9-weeks of age (Figure 1B). Insulin tolerance tests were performed in all four groups and Rag/MKR male and female mice demonstrated severe insulin resistance, with no glucose reduction in response to the 0.75Units/kg insulin injection over 60 minutes, while in Rag/WT control mice blood glucose levels rapidly fell greater to less than 50% of baseline, 60 minutes after the insulin injection (Figure 1C). The presence of endogenous hyperinsulinemia was confirmed by the measurement of non-fasting plasma insulin levels: 5.34ng/ml ± 0.45 in 9-week old female Rag/MKR mice compared with 1.01ng/ml ± 0.08 in Rag/WT female mice ($p<0.01$) and 11.7ng/ml ± 3.55 in 9 week old Rag/MKR males compared to 1.69ng/ml ± 0.31 in Rag/WT male mice (Figure 1D). Male Rag/MKR mice presented with endogenous hyperglycemia, assessed by the measurement of non-fasting blood glucose levels (Supplemental Figure 1A). Rag/MKR females present no signs of hyperglycemia, with non-fasting blood glucose levels comparable to Rag/WT male and female mice (Supplemental Figure 1A). Furthermore, a glucose tolerance test was performed on 8-week old mice after an 8 hour fast (Supplemental Figure 1B). The

Rag/MKR males were hyperglycemic, while the Rag/MKR females demonstrated mild glucose intolerance compared to Rag/WT females, consistent with them having insulin resistance (Supplemental Figure 1B). There was no difference in serum triglyceride or serum cholesterol levels between the Rag/WT and Rag/MKR mice (Supplemental Figure 1C and 1D). There was no significant difference in serum adiponectin or serum leptin levels in the Rag/WT and the Rag/MKR mice (Supplemental Figure 2A and 2B).

These results demonstrate that female MKR mice crossed with $Rag1^{-/-}$ mice are not obese, not hyperglycemic, nor dyslipidemic, but have insulin resistance with endogenous hyperinsulinemia and insulin levels that are approximately 5 times the control mice.

The role of the insulin receptor in the effect of hyperinsulinemia on human cancer progression

To examine the role of the insulin receptor (IR) in mediating the effect of the endogenous hyperinsulinemia on cancer progression, we studied the LCC6 IR6 clone cell line in which expression of the IR was markedly reduced by short hairpin RNA (Zhang et al. 2010) (Supplemental Figure 3). Tumors derived from LCC6 Ctrl cells grew more rapidly in Rag/MKR mice compared to Rag/WT LCC6 Ctrl cells, measuring 447.3 mm^3 ± 45.0 and 256.8 mm^3 ± 19.2, respectively, $p<0.05$ (Figure 2A). Tumors derived from the LCC6 IRKD cells were significantly smaller than their control cell counterparts (Figure 2A). Tumor weights were significantly greater in the Rag/MKR mice with Ctrl cells compared to Rag/WT mice with Ctrl cells 24 days after injection, weighing 0.31g ± 0.03 and 0.16g ± 0.01 respectively, $p<0.05$ (Figure 2B). The tumors from the LCC6 IRKD cells in the Rag/MKR and Rag/WT mice weighed 0.15g ± 0.02 and 0.07g ± 0.01 respectively, $p<0.05$ (Figure 2B). The reduction in tumor volume was seen both in Rag/WT and Rag/MKR mice. In both the Rag/WT mice and the Rag/MKR mice, the LCC6 IRKD tumor volume was decreased by half compared to respective Rag/WT and Rag/MKR with LCC6 Ctrl tumor volume.

Examining the IR Signaling Pathway

Sustained knockdown of the IR mRNA expression in the tumor xenografts was validated by qRT-PCR at the end of the study and an 83% reduction in *IR* expression was confirmed (Figure 3A). The *IGF1R* gene expression was decreased in the Rag/WT IRKD tumors, but there was no change in the *IGF1R* gene expression in the Rag/MKR Ctrl compared to the Rag/MKR IRKD tumors (Figure 3B). These results confirm successful knockdown of the insulin receptor in the cells and in the tumors generated in the Rag/WT and Rag/MKR mice.

Examining the insulin receptor signaling pathway, a significant decrease of phospho-AKT(Ser473) was observed in the IRKD tumors from both the Rag/WT and Rag/MKR mice (Figure 4A). Furthermore, an increase of phospho-AKT signaling was observed in the LCC6 Ctrl tumors from the Rag/MKR mice compared to the LCC6 Ctrl tumors from the Rag/WT mice (Figure 4A). There was a decrease in the phospho-S6 Ribosomal Protein (S6RP) in the IRKD tumors from both the Rag/WT and Rag/MKR mice (Figure 4B). Several studies have noted that insulin may have an effect on c-MYC expression (Ferguson et al. 2012; Mawson, et al. 2005) and that the phosphatidylinositol 3-kinse (PI3K) and mammalian target of

rapamycin (mTOR) signaling pathways may cooperate in regulating c-MYC expression (Sharma, et al. 2015). Analyzing the proteins from the primary tumors, we found that the LCC6 IRKD tumors had decreased c-MYC protein levels compared to LCC6 Ctrl tumors (Figure 4C). These results demonstrate that knockdown of the IR successfully decreases PI3K/AKT/mTOR signaling pathway, downstream targets of IR signaling. Furthermore, the data shows that reduction of IR signaling leads to a decrease of c-MYC protein levels.

Reversal of EMT in IRKD tumors

LCC6 Ctrl tumors in Rag/MKR mice had increased gene expression of *TWIST1* and *ZEB1* compared to Rag/WT Ctrl tumors (Figure 5A, B). The increased *SLUG* (SNAIL family transcription factor) gene expression in the LCC6 Ctrl tumors in the Rag/MKR mice compared to Rag/WT Ctrl tumors did not reach statistical significance (Figure 5C). The primary tumors from the Rag/MKR LCC6 Ctrl mice also had significantly higher levels of *VEGFA* compared to the primary tumors from the Rag/WT LCC6 Ctrl mice (Figure 5D). These results provide evidence that hyperinsulinemia promotes EMT and an increase in *VEGFA*, which may contribute to increased tumor growth and invasion in the Rag/MKR Ctrl tumors compared to the Rag/WT Ctrl tumors. Analyzing the LCC6 IRKD tumors, we found that gene expression of the mesenchymal transcription factors *TWIST1, ZEB1* and *SLUG* was reduced in the LCC6 IRKD tumors in both the Rag/WT and Rag/MKR mice (Figure 5A, B, C). The LCC6 IRKD tumors also had decreased levels of angiogenesis markers *VEGFA* (Figure 5D) and *VEGFD* (Supplemental Figure 4). The primary tumors from both the Rag/WT and Rag/MKR LCC6 IRKD cells had decreased protein levels of mesenchymal markers Vimentin, TWIST1 and SLUG compared to their LCC6 Ctrl tumors counterparts in the Rag/WT and Rag/MKR mice (Figure 6A, B, C). Furthermore, the LCC6 IRKD primary tumors re-expressed E-cadherin, a classic epithelial marker (Figure 6D). The knockdown of the IR promoted a reversal of the epithelial-mesenchymal transition by repressing mesenchymal markers and re-expressing epithelial markers in the LCC6 IRKD tumors.

IRKD clone had decreased number of lung metastases in hyperinsulinemic mice

The LCC6 orthotopically injected cells have been shown to metastasize to the lungs. The lungs harvested 28 days post cancer cell inoculation were sectioned and examined for micrometastasis. In the Rag/WT mice, neither the mice with the LCC6 Ctrl tumors (0/5) nor the mice with the LCC6 IRKD tumors (0/5) had any pulmonary micrometastases. In the lungs from the hyperinsulinemic Rag/MKR group, 2/5 (40%) of the mice with LCC6 Ctrl tumors had numerous lung micrometastases (Figure 7), while 0/5 (0%) lungs from the Rag/MKR mice with LCC6 IRKD tumors had micrometastasis. The data suggest that silencing the insulin receptor diminished cancer cell metastasis to the lung of the hyperinsulinemic mice, likely through the down-regulation of mesenchymal proteins.

Discussion

Epidemiological studies have demonstrated the association between obesity and Type 2 diabetes and an increased cancer risk and mortality of both epithelial such as colon, breast, endometrial cancers and non-solid tumors, such as lymphomas (Haslam and James 2005;

Onitilo et al. 2012). Of the numerous potential factors that could explain this association, endogenous hyperinsulinemia has been identified as an important factor inversely correlating with survival in women with breast cancer (Eliassen et al. 2007; Goodwin et al. 2002). To determine whether endogenous hyperinsulinemia is a direct causal factor in promoting progression of human tumors, by acting on the tumor cell IR, we have generated a novel immunodeficient mouse model of endogenous hyperinsulinemia, the female Rag/MKR mouse that (unlike the male mouse that shows the full phenotype of Type 2 diabetes) exhibits severe insulin resistance and hyperinsulinemia, without hyperglycemia. This mouse thus represents the equivalent of the insulin resistance and endogenous hyperinsulinemia seen in obesity and pre-diabetes without the other confounding variables, such as dyslipidemia or the need for a high fat diet. In fact, the Rag/MKR mice have lower body weight, lower fat mass, normal triglyceride, normal cholesterol and normal adiponectin levels compared to Rag/WT control mice. It would be expected that a decrease in fat mass would also show a decrease in leptin levels. In a previously published study from our group, we found that in MKR females there were lower leptin levels (Fierz, et al. 2010a), while in MKR males there was no significant difference compared with control mice (Toyoshima, et al. 2005). In the current study, the Rag/MKR female mice had no significant difference in leptin levels compared with control mice, which may be due to the large error bars in the Rag/WT female group. The work in this paper demonstrated that we successfully generated an immunodeficient mouse model of both Type 2 diabetes (male mice) and pre-diabetes (female mice). The difference between the degree of severity of diabetes between the male and female mice, is likely attributed to estrogen in the female mice. In immunocompetent hyperinsulinemic MKR mice, ovariectomy led to the female MKR mice to develop additional symptoms of Type 2 diabetes (hypercholesterolemia and hyperglycemia) (Ben-Shmuel, et al. 2015). In other animal models, estrogen has been shown to reverse the adverse metabolic effects of ovariectomy (Zhu, et al. 2013).

Similar to our previous studies, using mouse mammary tumors (Ferguson et al. 2012; Fernandez et al. 2001; Novosyadlyy et al. 2010), we have found that the Rag/MKR mice develop larger primary tumors with more numerous pulmonary metastasis when injected with human metastatic LCC6 cells (a variant of MDA-MB-435) that are highly malignant and metastasize (Holliday and Speirs 2011; Price 1996). In our previous studies on murine cancers, we found that increased tumor promotion was reversed when the IR/IGF1Rs were blocked using a tyrosine kinase inhibitor or the hyperinsulinemia was pharmacologically reduced, thereby suggesting a role for insulin and the IR/IGF1R in tumor progression (Ferguson et al. 2012; Fierz et al. 2010a; Fierz, et al. 2010b; Gallagher, et al. 2012; Novosyadlyy et al. 2010). However, in these studies we could not examine the effects of hyperinsulinemia on human cancers.

It has previously been shown that constitutive activation of the IGF1R in non-transformed human mammary epithelial cells promoted increased proliferation, loss of contact inhibition, anchorage-independent growth, invasion and tumorigenesis (Kim, et al. 2007). The MCF10A cells up-regulated SNAIL mRNA levels (a mesenchymal transcription factor) and down-regulated E-Cadherin mRNA levels in response to IGF1R over-expression (Kim et al. 2007). Using a small molecule inhibitor of IGF1R/IR reversed the EMT changes caused by the IGF1R overexpression in the MCF10A cells; an increase in E-cadherin mRNA levels

was observed, as well as a decrease in the mesenchymal marker vimentin (Kim et al. 2007). The study by Kim *et al* did not examine the expression of the IR in the setting of IGF1R over-expression. Our current study demonstrates that the female Rag/MKR mouse has more aggressive tumor growth compared to the Rag/WT mice. The data indicates that the IR expression on the tumor cells is important for tumor growth. However, in the Rag/MKR mice with the IRKD tumors, there was still an increase in tumor growth compared to the Rag/WT IRKD tumors. This may indicate that tumor growth may be mediated by the hyperinsulinemia in the Rag/MKR mice acting directly or indirectly, potentially by regulating IGFBP expression and local bioavailable IGF1 levels. The EMT changes seen in the Rag/MKR mice appear to be mediated directly by the effects of insulin on the insulin receptor. We have previously shown that in the MKR hyperinsulinemic mice there is an up-regulation of both the IR and IGF1R expression in the tumors compared to the tumors from control mice (Ferguson et al. 2012). The LCC6 IR knockdown tumors in the Rag/MKR mice have higher level of IGF1R than the LCC6 IR knockdown tumors from the Rag/WT mice. This could partially compensate for the IR knockdown in the Rag/MKR mice. Therefore, in the absence of the IR, hyperinsulinemia may promote tumor growth by acting directly or indirectly through the IGF1R.

The Rag/MKR LCC6 Ctrl primary tumors show elevated AKT/mTOR signaling, increased EMT gene expression of *TWIST1* and *ZEB1*, and increased gene expression of *VEGFA* compared to the Rag/WT LCC6 Ctrl tumors. All of these factors may contribute to the increased tumor growth in the Rag/MKR mice. We have previously found an increase in phospho-AKT signaling in the primary tumors from MKR mice compared to controls and that inhibiting PI3K/AKT signaling reduces murine tumor growth (Gallagher et al. 2012; Novosyadlyy et al. 2010). Using the LCC6 IRKD cells we demonstrated that the IRKD significantly reverses the effect of the hyperinsulinemia and that the tumors from the IRKD cells are significantly smaller in both the Rag/WT and Rag/MKR mice compared to the LCC6 Ctrl counterparts, and have less metastatic lesions. Moreover, we show that the Rag/MKR LCC6 Ctrl primary tumors have increased expression of *VEGFA* and *VEGFD*. *VEGFA* and *VEGFD* are known mediator of angiogenesis that has been linked to tumor growth (Calvo, et al. 2008; Zhang, et al. 2007). In previously published work from the lab, we found that there were increased levels of VEGF and in tumors from the MKR mice (Ferguson et al. 2012). The increased expression of VEGF may indicate increased angiogenesis, an important process in tumor growth and metastasis (Calvo et al. 2008; Zhang et al. 2007). The increased gene expression of *VEGFA* and *VEGFD* may contribute to the increased tumor size and numerous metastases in the hyperinsulinemic LCC6 Ctrl mice.

We show that IRKD leads to significant decreases in phospho-AKT, phospho-S6RP and in the expression of the cancer growth enhancing protein c-MYC. c-MYC is a transcription factor that is known to control cell cycle progression and differentiation (Xu, et al. 2010). Approximately 50% of breast cancers are due to an oncogenic transformation, which leads to an overexpression of c-MYC either through gene amplification, chromosomal transformation or protein overexpression events (Chrzan, et al. 2001; Xu et al. 2010). It has been shown that using the dual PI3K/mTOR inhibitor NVP-BEZ235 inhibits the expression of c-MYC in pancreatic cancer cells (Sharma et al. 2015). Moreover, c-MYC has also been

linked to promoting EMT induction in endometrial cancer cells (Liu, et al. 2015). Therefore, the decrease in c-MYC protein expression in the IRKD tumors in both the Rag/WT and Rag/MKR mice may contribute to the significantly decreased tumor sizes and reversal of EMT in the tumors of those mice. Furthermore, the down-regulation of the IR in the LCC6 cells significantly affected the formation of colonies in soft agar (Zhang et al. 2010). These results highlight the importance of the insulin receptor in proliferation and the reversal of EMT may explain their inability to overcome anoikis.

The parent of the LCC6 cells, the MDA-MB-435 cell line, is highly metastatic and expresses many of the classic EMT markers such as low levels of E-cadherin and high levels of Vimentin, N-cadherin, and alpha smooth muscle actin (Li, et al. 2014; Manni, et al. 2002). In the current study, we show down-regulated expression of mesenchymal markers including Vimentin, TWIST1, SLUG (SNAIL family transcription factor) and ZEB1 at RNA and protein levels in the tumors with IR knockdown. While we saw an increase in *TWIST1 and SLUG* gene expression in the Rag/MKR Ctrl tumors compared to the Rag/WT Ctrl tumors, we did not see a significant difference in the protein levels of these genes between the Rag/MKR Ctrl and Rag/WT Ctrl tumors. This may be in part due to the short half-life of the TWIST and SNAIL transcription factor family proteins that are rapidly polyubiquitinated and degraded by the proteasome in cells (Diaz, et al. 2014). These mesenchymal factors are essential markers of EMT, a biological process in which polarized-epithelial cells undergo various changes to take on a mesenchymal phenotype. This phenotype includes increased migratory capacity, invasiveness, resistance to apoptosis, and elevated production of extracellular matrix (ECM) components (Kalluri and Weinberg 2009; Thiery 2002). In many carcinomas, growth factors such as transforming growth factor-beta (TGFB) and epidermal growth factor (EGF), can lead to the induction of EMT signals by increasing the gene expression of various EMT-inducing transcription factors; most commonly SNAIL, SLUG, zinc finger E-box binding homeobox 1 (ZEB1), and TWIST1 (Al Moustafa, et al. 2012; Kim, et al. 2002; Niessen, et al. 2008; Pan, et al. 2012; Shi and Massague 2003; Spaderna, et al. 2008). The data presented in this study is the first to our knowledge to show that hyperinsulinemia increases the expression of several EMT genes in vivo. ZEB1 has been shown to induce EMT and down-regulate E-cadherin in epithelial cells (Singh, et al. 2008). Moreover, ZEB1 knockdown in non-small cell lung cancer cell lines suppressed the growth and colony formation of the cells (Takeyama, et al. 2010). In the same study, they noted that ZEB1 knockdown induced E-cadherin mRNA expression in some of the non-small cell lung cancer cell lines (Takeyama et al. 2010). It has been shown that re-expression of E-cadherin can partially revert mesenchymal breast cancer cells toward an epithelial phenotype, as well as suppress migration and invasion of the cells (Chao, et al. 2010).

In previously published data, it has been shown that the parent LCC6 cells readily metastasize in athymic mice (Zhang et al. 2010). In our current study we show that the LCC6 Ctrl cells did not metastasize in the Rag/WT mice, but did metastasize in the Rag/MKR mice. The discrepancy between the previous published data and the lack of metastases in the Rag/WT mice in the current study may relate to either differences in the mouse strains or the time to assess the number of pulmonary metastases. However, it is important to note that the LCC6 Ctrl primary tumors of the Rag/MKR mice showed increased levels of phospho-AKT and higher gene expression of *TWIST1, ZEB1* and

VEGFA compared to the LCC6 Ctrl tumors of Rag/WT mice, which can contribute to the increased tumor growth and metastases seen in the Rag/MKR LCC6 Ctrl tumors. The data presented in this study also show that insulin receptor knockdown leads to a decrease in ZEB1 transcriptional activity, which promotes the re-expression of E-cadherin, which was not previously showed by Zhang *et al*. This may lead to decreased colony formation and decreased number of pulmonary metastasis formation.

In summary, we demonstrate that the female Rag/MKR mouse model is a novel immunodeficient model for pre-diabetes. This mouse model can be used to study many other human tumor types where hyperinsulinemia may play a role. The current study showed that silencing the insulin receptor in the LCC6 tumor cells decreased the tumor growth in both the Rag/WT and Rag/MKR mice. We show for the first time that hyperinsulinemic mice have increased EMT gene expression, increased VEGFA expression, and have more pulmonary metastases. We also show for the first time that silencing the insulin receptor leads to a reversal of the EMT phenotype where these tumors were able to re-express E-cadherin and down-regulate Vimentin, TWIST1, SLUG, and ZEB1 expression. Furthermore, the tumors from the insulin receptor knockdown cells had significantly decreased phospho-AKT and c-MYC expression, even in the setting of hyperinsulinemia. This suggests that reducing insulin receptor signaling or expression specifically in the tumors may lead to reduced number of pulmonary metastases.

Supplementary Material

Refer to Web version on PubMed Central for supplementary material.

Acknowledgments

Funding

This work was supported by the NIH/NCI grant (2R01CA128799-06A1) and American Diabetes Association grant (1-13-BS-108) to Dr. Derek LeRoith and the NIH/NCI grant 1K08CA190770 to Dr. Emily Jane Gallagher.

References

Al Moustafa AE, Achkhar A, Yasmeen A. EGF-receptor signaling and epithelial-mesenchymal transition in human carcinomas. Front Biosci (Schol Ed). 2012; 4:671–684. [PubMed: 22202084]

Alikhani N, Ferguson RD, Novosyadlyy R, Gallagher EJ, Scheinman EJ, Yakar S, LeRoith D. Mammary tumor growth and pulmonary metastasis are enhanced in a hyperlipidemic mouse model. Oncogene. 2013; 32:961–967. [PubMed: 22469977]

Ben-Shmuel S, Scheinman EJ, Rashed R, Orr ZS, Gallagher EJ, LeRoith D, Rostoker R. Ovariectomy is associated with metabolic impairments and enhanced mammary tumor growth in MKR mice. J Endocrinol. 2015; 227:143–151. [PubMed: 26383532]

Calvo A, Catena R, Noble MS, Carbott D, Gil-Bazo I, Gonzalez-Moreno O, Huh JI, Sharp R, Qiu TH, Anver MR, et al. Identification of VEGF-regulated genes associated with increased lung metastatic potential: functional involvement of tenascin-C in tumor growth and lung metastasis. Oncogene. 2008; 27:5373–5384. [PubMed: 18504437]

Chambers AF. MDA-MB-435 and M14 cell lines: identical but not M14 melanoma? Cancer Res. 2009; 69:5292–5293. [PubMed: 19549886]

Chao YL, Shepard CR, Wells A. Breast carcinoma cells re-express E-cadherin during mesenchymal to epithelial reverting transition. Mol Cancer. 2010; 9:179. [PubMed: 20609236]

Chrzan P, Skokowski J, Karmolinski A, Pawelczyk T. Amplification of c-myc gene and overexpression of c-Myc protein in breast cancer and adjacent non-neoplastic tissue. Clin Biochem. 2001; 34:557–562. [PubMed: 11738392]

DeFuria J, Belkina AC, Jagannathan-Bogdan M, Snyder-Cappione J, Carr JD, Nersesova YR, Markham D, Strissel KJ, Watkins AA, Zhu M, et al. B cells promote inflammation in obesity and type 2 diabetes through regulation of T-cell function and an inflammatory cytokine profile. Proc Natl Acad Sci U S A. 2013; 110:5133–5138. [PubMed: 23479618]

Diaz VM, Vinas-Castells R, Garcia de Herreros A. Regulation of the protein stability of EMT transcription factors. Cell Adh Migr. 2014; 8:418–428. [PubMed: 25482633]

Eliassen AH, Tworoger SS, Mantzoros CS, Pollak MN, Hankinson SE. Circulating insulin and c-peptide levels and risk of breast cancer among predominately premenopausal women. Cancer Epidemiol Biomarkers Prev. 2007; 16:161–164. [PubMed: 17220346]

Ferguson RD, Novosyadlyy R, Fierz Y, Alikhani N, Sun H, Yakar S, Leroith D. Hyperinsulinemia enhances c-Myc-mediated mammary tumor development and advances metastatic progression to the lung in a mouse model of type 2 diabetes. Breast Cancer Res. 2012; 14:R8. [PubMed: 22226054]

Fernandez AM, Kim JK, Yakar S, Dupont J, Hernandez-Sanchez C, Castle AL, Filmore J, Shulman GI, Le Roith D. Functional inactivation of the IGF-I and insulin receptors in skeletal muscle causes type 2 diabetes. Genes Dev. 2001; 15:1926–1934. [PubMed: 11485987]

Fierz Y, Novosyadlyy R, Vijayakumar A, Yakar S, LeRoith D. Insulin-sensitizing therapy attenuates type 2 diabetes-mediated mammary tumor progression. Diabetes. 2010a; 59:686–693. [PubMed: 19959755]

Fierz Y, Novosyadlyy R, Vijayakumar A, Yakar S, LeRoith D. Mammalian target of rapamycin inhibition abrogates insulin-mediated mammary tumor progression in type 2 diabetes. Endocr Relat Cancer. 2010b; 17:941–951. [PubMed: 20801951]

Gallagher EJ, Fierz Y, Vijayakumar A, Haddad N, Yakar S, LeRoith D. Inhibiting PI3K reduces mammary tumor growth and induces hyperglycemia in a mouse model of insulin resistance and hyperinsulinemia. Oncogene. 2012; 31:3213–3222. [PubMed: 22037215]

Goodwin PJ, Ennis M, Pritchard KI, Trudeau ME, Koo J, Madarnas Y, Hartwick W, Hoffman B, Hood N. Fasting insulin and outcome in early-stage breast cancer: results of a prospective cohort study. J Clin Oncol. 2002; 20:42–51. [PubMed: 11773152]

Haslam DW, James WP. Obesity. Lancet. 2005; 366:1197–1209. [PubMed: 16198769]

Holliday DL, Speirs V. Choosing the right cell line for breast cancer research. Breast Cancer Res. 2011; 13:215. [PubMed: 21884641]

Howe LR, Subbaramaiah K, Hudis CA, Dannenberg AJ. Molecular pathways: adipose inflammation as a mediator of obesity-associated cancer. Clin Cancer Res. 2013; 19:6074–6083. [PubMed: 23958744]

Hursting SD, Digiovanni J, Dannenberg AJ, Azrad M, Leroith D, Demark-Wahnefried W, Kakarala M, Brodie A, Berger NA. Obesity, energy balance, and cancer: new opportunities for prevention. Cancer Prev Res (Phila). 2012; 5:1260–1272. [PubMed: 23034147]

Kalluri R, Weinberg RA. The basics of epithelial-mesenchymal transition. J Clin Invest. 2009; 119:1420–1428. [PubMed: 19487818]

Kim HJ, Litzenburger BC, Cui X, Delgado DA, Grabiner BC, Lin X, Lewis MT, Gottardis MM, Wong TW, Attar RM, et al. Constitutively active type I insulin-like growth factor receptor causes transformation and xenograft growth of immortalized mammary epithelial cells and is accompanied by an epithelial-to-mesenchymal transition mediated by NF-kappaB and snail. Mol Cell Biol. 2007; 27:3165–3175. [PubMed: 17296734]

Kim K, Lu Z, Hay ED. Direct evidence for a role of beta-catenin/LEF-1 signaling pathway in induction of EMT. Cell Biol Int. 2002; 26:463–476. [PubMed: 12095232]

Li J, Liu J, Li P, Mao X, Li W, Yang J, Liu P. Loss of LKB1 disrupts breast epithelial cell polarity and promotes breast cancer metastasis and invasion. J Exp Clin Cancer Res. 2014; 33:70. [PubMed: 25178656]

Liu L, Zhang J, Yang X, Fang C, Xu H, Xi X. SALL4 as an Epithelial-Mesenchymal Transition and Drug Resistance Inducer through the Regulation of c-Myc in Endometrial Cancer. PLoS One. 2015; 10:e0138515. [PubMed: 26407074]

Manni A, Washington S, Griffith JW, Verderame MF, Mauger D, Demers LM, Samant RS, Welch DR. Influence of polyamines on in vitro and in vivo features of aggressive and metastatic behavior by human breast cancer cells. Clin Exp Metastasis. 2002; 19:95–105. [PubMed: 11964084]

Mawson A, Lai A, Carroll JS, Sergio CM, Mitchell CJ, Sarcevic B. Estrogen and insulin/IGF-1 cooperatively stimulate cell cycle progression in MCF-7 breast cancer cells through differential regulation of c-Myc and cyclin D1. Mol Cell Endocrinol. 2005; 229:161–173. [PubMed: 15607540]

Mombaerts P, Iacomini J, Johnson RS, Herrup K, Tonegawa S, Papaioannou VE. RAG-1-deficient mice have no mature B and T lymphocytes. Cell. 1992; 68:869–877. [PubMed: 1547488]

Morris DL, Cho KW, Delproposto JL, Oatmen KE, Geletka LM, Martinez-Santibanez G, Singer K, Lumeng CN. Adipose tissue macrophages function as antigen-presenting cells and regulate adipose tissue CD4+ T cells in mice. Diabetes. 2013; 62:2762–2772. [PubMed: 23493569]

Niessen K, Fu Y, Chang L, Hoodless PA, McFadden D, Karsan A. Slug is a direct Notch target required for initiation of cardiac cushion cellularization. J Cell Biol. 2008; 182:315–325. [PubMed: 18663143]

Novosyadlyy R, Lann DE, Vijayakumar A, Rowzee A, Lazzarino DA, Fierz Y, Carboni JM, Gottardis MM, Pennisi PA, Molinolo AA, et al. Insulin-mediated acceleration of breast cancer development and progression in a nonobese model of type 2 diabetes. Cancer Res. 2010; 70:741–751. [PubMed: 20068149]

Onitilo AA, Engel JM, Glurich I, Stankowski RV, Williams GM, Doi SA. Diabetes and cancer I: risk, survival, and implications for screening. Cancer Causes Control. 2012; 23:967–981. [PubMed: 22552844]

Pan B, Ren H, He Y, Lv X, Ma Y, Li J, Huang L, Yu B, Kong J, Niu C, et al. HDL of patients with type 2 diabetes mellitus elevates the capability of promoting breast cancer metastasis. Clin Cancer Res. 2012; 18:1246–1256. [PubMed: 22261802]

Price JE. Metastasis from human breast cancer cell lines. Breast Cancer Res Treat. 1996; 39:93–102. [PubMed: 8738609]

Sharma N, Nanta R, Sharma J, Gunewardena S, Singh KP, Shankar S, Srivastava RK. PI3K/AKT/mTOR and sonic hedgehog pathways cooperate together to inhibit human pancreatic cancer stem cell characteristics and tumor growth. Oncotarget. 2015; 6:32039–32060. [PubMed: 26451606]

Shi Y, Massague J. Mechanisms of TGF-beta signaling from cell membrane to the nucleus. Cell. 2003; 113:685–700. [PubMed: 12809600]

Singh M, Spoelstra NS, Jean A, Howe E, Torkko KC, Clark HR, Darling DS, Shroyer KR, Horwitz KB, Broaddus RR, et al. ZEB1 expression in type I vs type II endometrial cancers: a marker of aggressive disease. Mod Pathol. 2008; 21:912–923. [PubMed: 18487993]

Spaderna S, Schmalhofer O, Wahlbuhl M, Dimmler A, Bauer K, Sultan A, Hlubek F, Jung A, Strand D, Eger A, et al. The transcriptional repressor ZEB1 promotes metastasis and loss of cell polarity in cancer. Cancer Res. 2008; 68:537–544. [PubMed: 18199550]

Takeyama Y, Sato M, Horio M, Hase T, Yoshida K, Yokoyama T, Nakashima H, Hashimoto N, Sekido Y, Gazdar AF, et al. Knockdown of ZEB1, a master epithelial-to-mesenchymal transition (EMT) gene, suppresses anchorage-independent cell growth of lung cancer cells. Cancer Lett. 2010; 296:216–224. [PubMed: 20452118]

Thiery JP. Epithelial-mesenchymal transitions in tumour progression. Nat Rev Cancer. 2002; 2:442–454. [PubMed: 12189386]

Toyoshima Y, Gavrilova O, Yakar S, Jou W, Pack S, Asghar Z, Wheeler MB, LeRoith D. Leptin improves insulin resistance and hyperglycemia in a mouse model of type 2 diabetes. Endocrinology. 2005; 146:4024–4035. [PubMed: 15947005]

Xu J, Chen Y, Olopade OI. MYC and Breast Cancer. Genes Cancer. 2010; 1:629–640. [PubMed: 21779462]

Zhang H, Fagan DH, Zeng X, Freeman KT, Sachdev D, Yee D. Inhibition of cancer cell proliferation and metastasis by insulin receptor downregulation. Oncogene. 2010; 29:2517–2527. [PubMed: 20154728]

Zhang J, Lu A, Beech D, Jiang B, Lu Y. Suppression of breast cancer metastasis through the inhibition of VEGF-mediated tumor angiogenesis. Cancer Ther. 2007; 5:273–286. [PubMed: 18548129]

Zhang PH, Chen ZW, Lv D, Xu YY, Gu WL, Zhang XH, Le YL, Zhu HH, Zhu YM. Increased risk of cancer in patients with type 2 diabetes mellitus: A retrospective cohort study in China. BMC Public Health. 2012; 12:567. [PubMed: 22839452]

Zhu L, Brown WC, Cai Q, Krust A, Chambon P, McGuinness OP, Stafford JM. Estrogen treatment after ovariectomy protects against fatty liver and may improve pathway-selective insulin resistance. Diabetes. 2013; 62:424–434. [PubMed: 22966069]

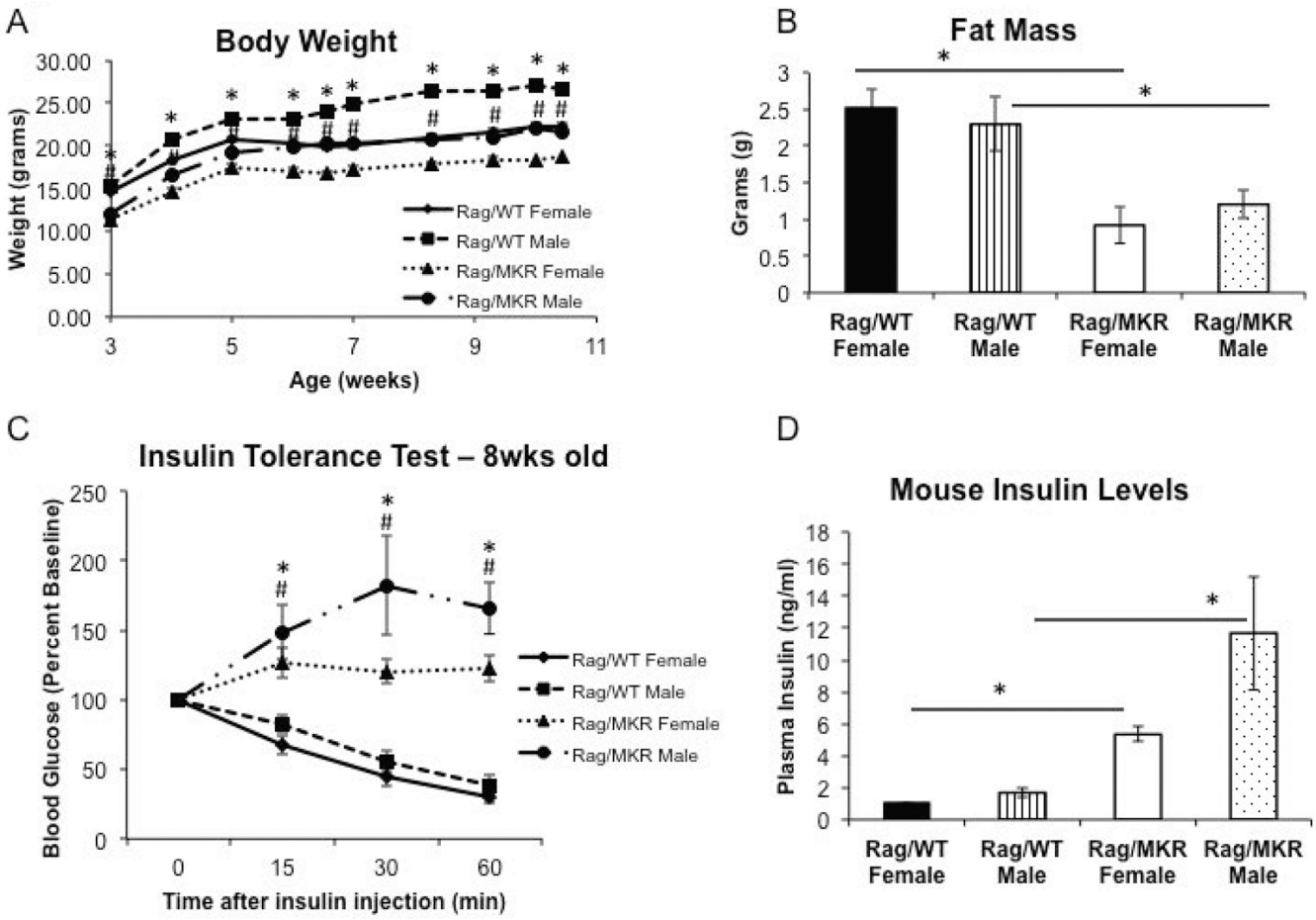

Figure 1.

Characterization of an immunodeficient hyperinsulinemic mouse model. (A) Body weights of male and female mice from Rag/WT and Rag/MKR mice, measured weekly from 3 weeks of age to 10 weeks of age. * $p<0.05$ between Rag/WT male and Rag/MKR male mice. # $p<0.05$ between Rag/WT female and Rag/MKR female mice. N=5 mice per group, error bars represent SEM. (B) MRI results showing whole body fat in Rag/WT and Rag/MKR mice. N=5 mice per group, error bars represent SEM. (C) Insulin Tolerance Test (ITT) performed on fasted 8 week male and female Rag/WT and Rag/MKR mice. Blood glucose levels were measured at time 0 and 15, 30, and 60 minutes post insulin injection. Mice were injected with 0.75U/kg insulin. * $p<0.05$ between Rag/WT male and Rag/MKR male mice. # $p<0.05$ between Rag/WT female and Rag/MKR female mice. N=5 mice per group, error bars represent SEM. (D) Plasma insulin levels of non-fasted male and female Rag/WT and Rag/MKR mice. * $p<0.05$ between groups as indicated. Graphs represent the mean of each group (n=5 mice per group), error bars are SEM.

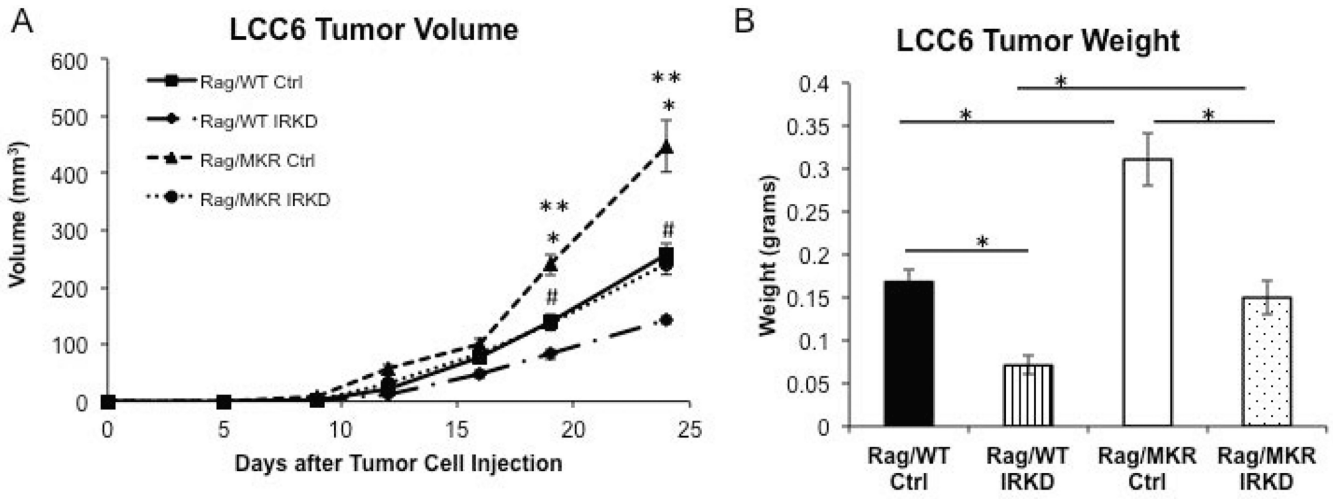

Figure 2.

Silencing the insulin receptor leads to decreased tumor growth. 8–10 week old Rag/WT control and Rag/MKR hyperinsulinemic mice were injected with either 5×10^6 LCC6 control (Ctrl) or 5×10^6 LCC6 insulin receptor knockdown (IRKD) cells, into the 4th mammary fat pad (n=8–10 mice per group). (A) Mammary tumor volume was calculated from tumor measurements taken twice weekly with calipers. * $p<0.05$ between Rag/MKR Ctrl and Rag/WT Ctrl tumors. ** $p<0.05$ between Rag/MKR Ctrl and Rag/MKR IRKD. # $p<0.05$ between Rag/WT Ctrl and Rag/WT IRKD tumors. N=8–10 mice per group, error bars represent SEM. (B) Tumor weight at the end of the study. (* $p<0.05$ between groups as indicated). N=8–10 mice per group, error bars represent SEM.

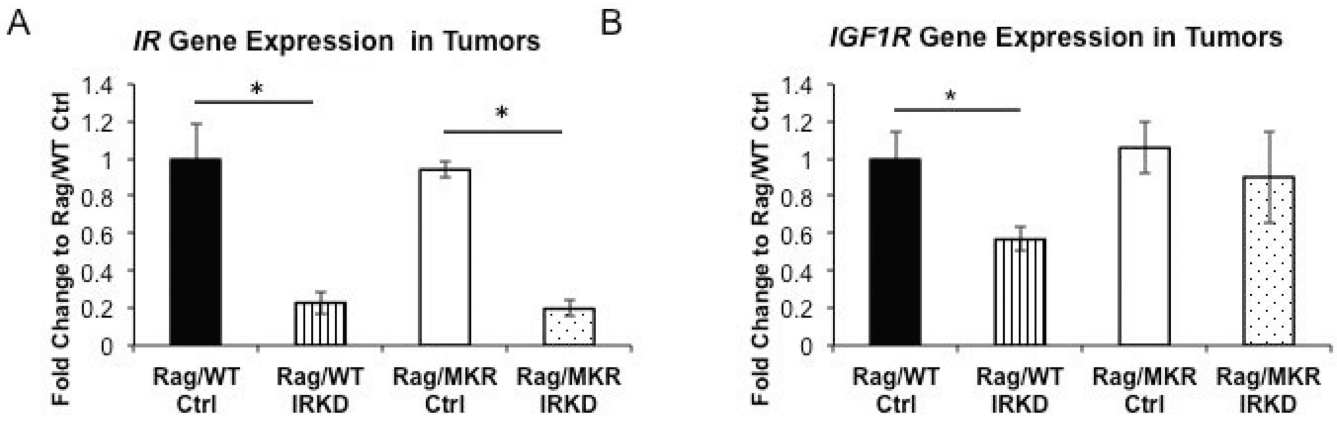

Figure 3.

Expression of *IR* and *IGF1R* in LCC6 Tumors. (A) Primary tumors from Rag/WT and Rag/MKR mice were assessed for the gene expression of the insulin receptor, demonstrating an 83% reduction of *IR* in the tumors from the LCC6 IRKD cells. (* $p<0.05$, n=8–10 mice per group, error bars represent SEM.). (B) Primary tumors from Rag/WT and Rag/MKR mice were assessed for the gene expression of the insulin like growth factor-1 receptor *IGF1R* (* $p<0.05$ n=8–10 mice per group, error bars are SEM.)

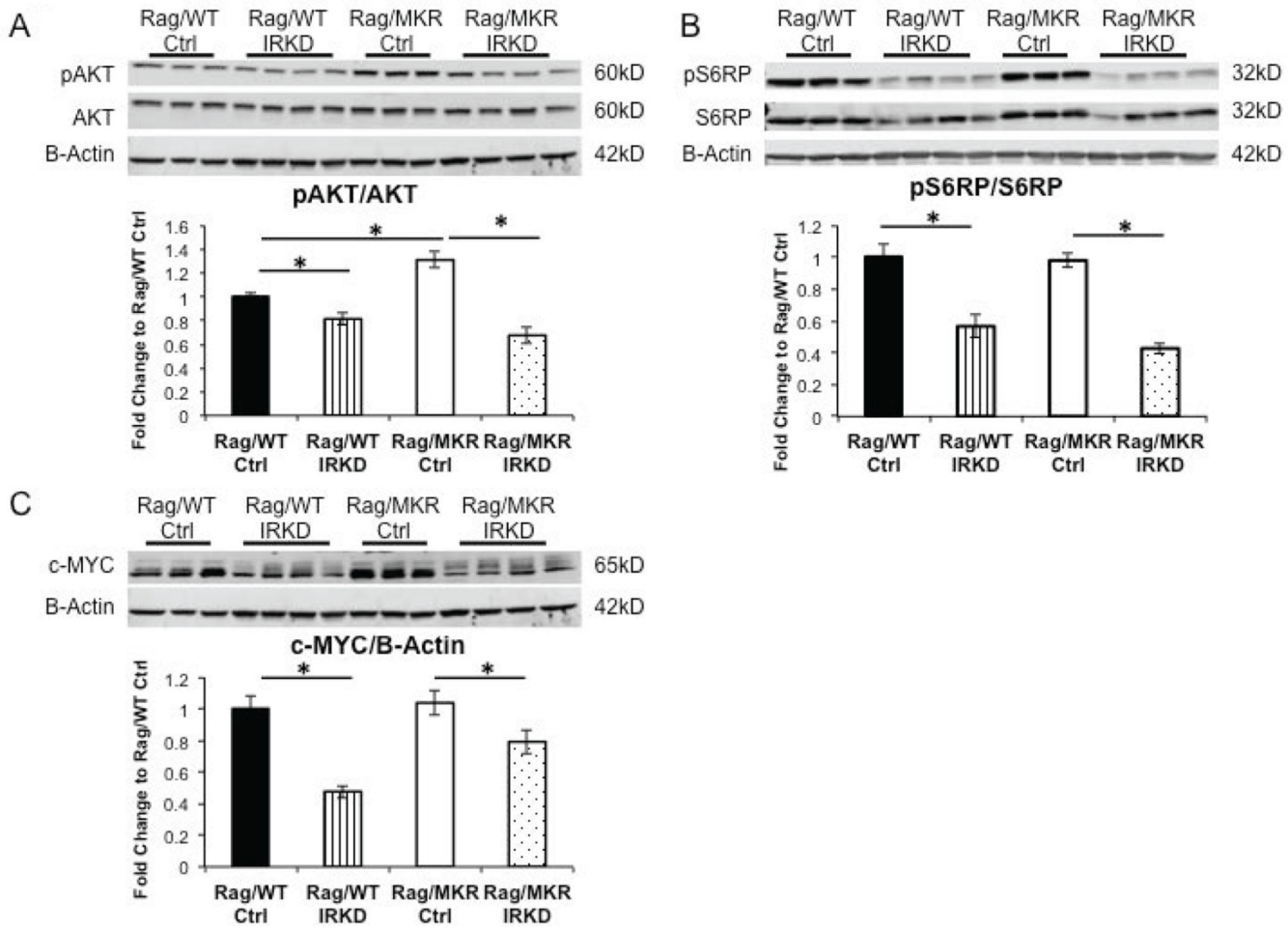

Figure 4.

Reduction of insulin signaling pathway in LCC6 IRKD tumors. (A) Representative blots showing protein extracted from tumor tissue and analyzed by Western blot for phospho-Akt (pAKT) and total AKT expression. B-Actin antibody used as loading control. Densitometry of Western blot (* $p<0.05$, graphs represent mean per group (n=8–10 mice per group) and error bars represent SEM). (B) Representative blots showing protein extracted from tumor tissue and analyzed by Western blot for phospho-S6 ribosomal protein (pS6RP) and total S6RP expression. B-Actin antibody used as loading control. Densitometry of Western blot (* $p<0.05$, graphs represent mean per group (n=8–10 mice per group) and error bars represent SEM). (C) Representative blots showing protein extracted from tumor tissue and analyzed by Western blot for c-MYC expression. B-Actin antibody was used as the loading control. Densitometry of Western blot of c-MYC/B-Actin (* $p<0.05$, graphs represent mean per group (n=8–10 mice per group) and error bars are SEM).

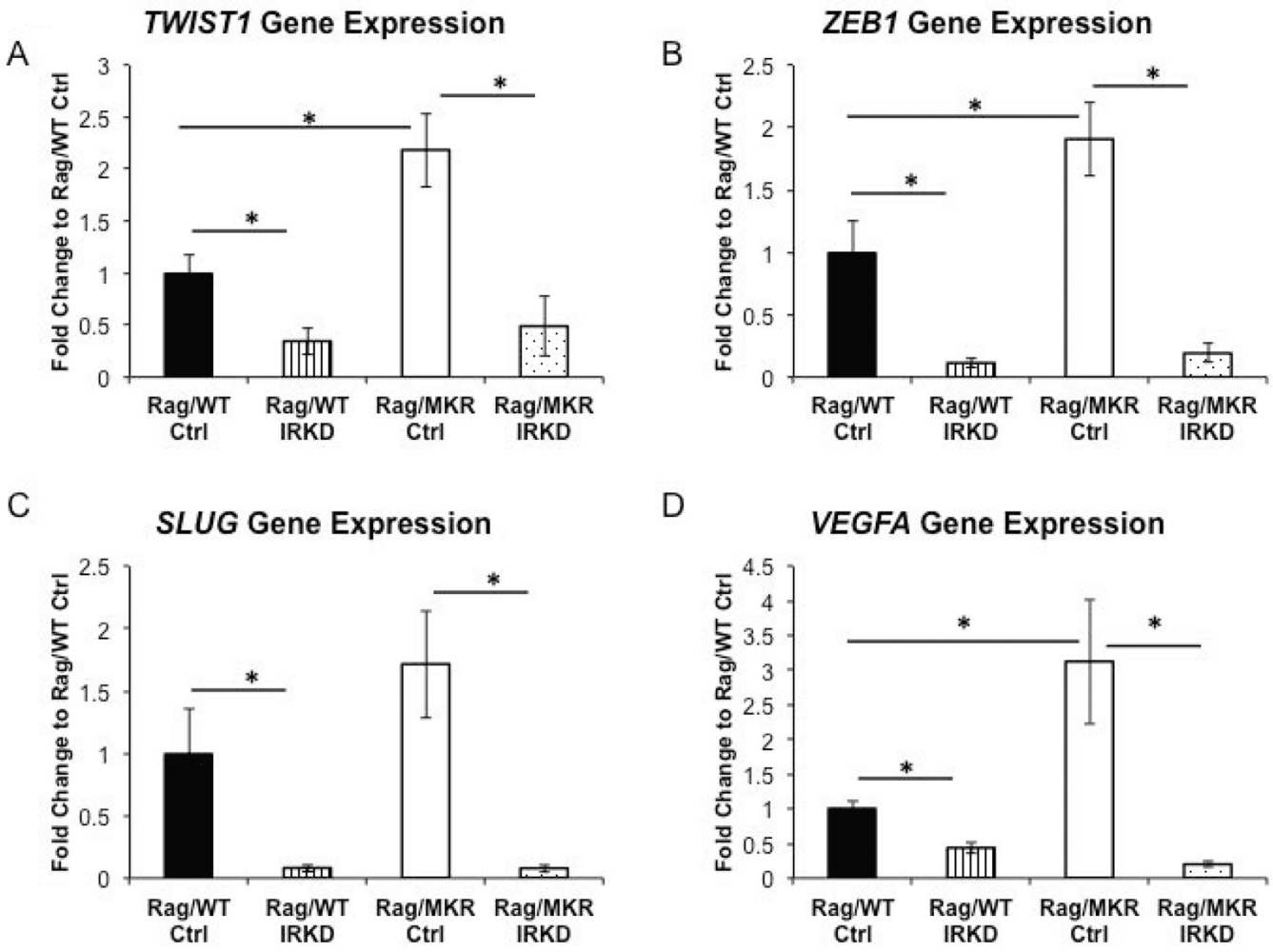

Figure 5.

EMT and angiogenesis in Ctrl and IRKD tumors. RNA extracted from tumor tissue was analyzed for (A) *TWIST1*, (B) *ZEB1*, (C) *SLUG*, and (D) Vascular endothelial growth factor A (*VEGFA*) gene expression by qRT-PCR. Calculations were made using ribosomal protein L19 (RPL19) as housekeeping gene. Graphs represent mean per group (n=5 per group) and error bars are SEM. (* $p<0.05$).

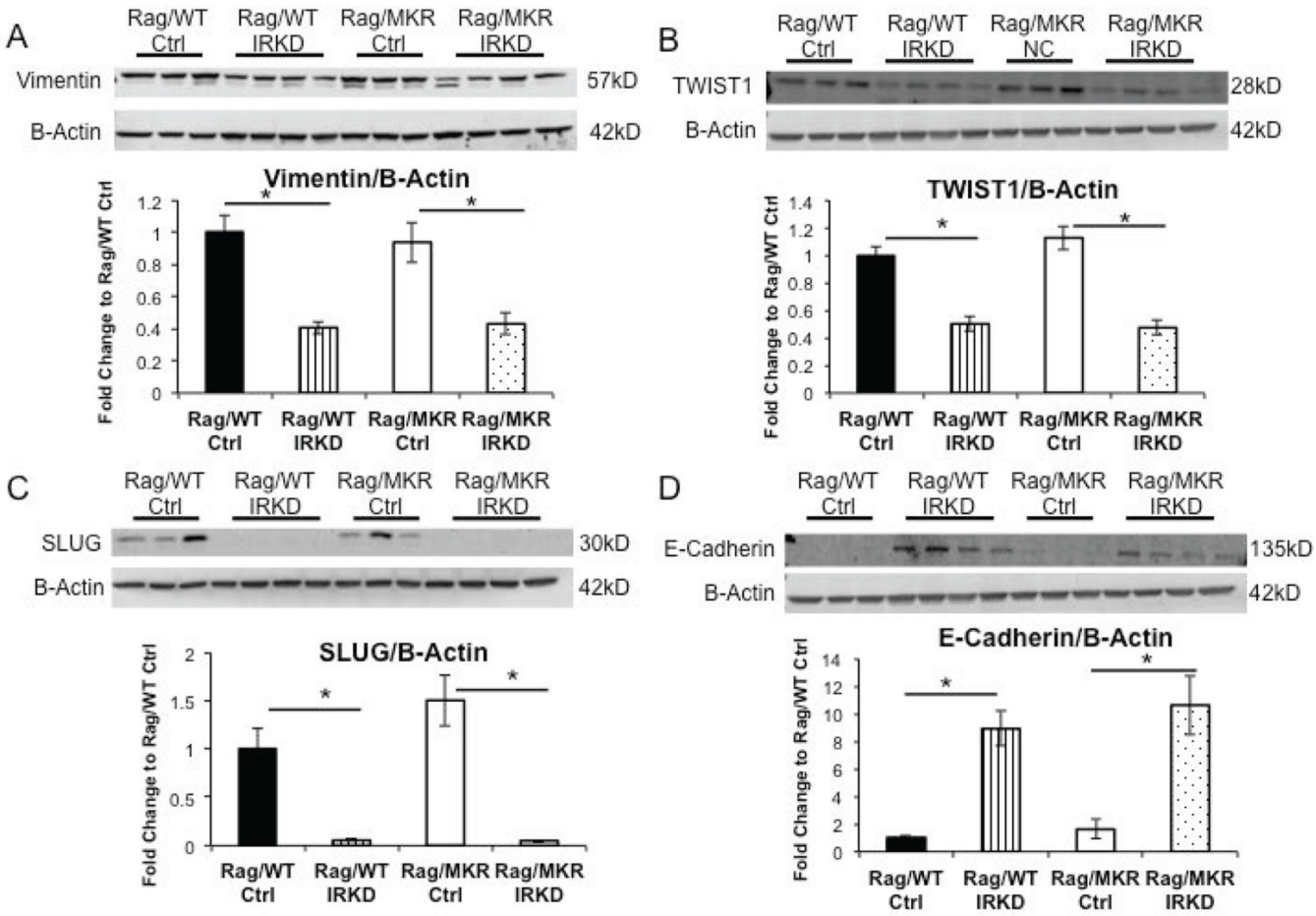

Figure 6.

Tumors from LCC6 IRKD cells have reversal of Epithelial-Mesenchymal Transition phenotype. (A) Representative blots showing protein extracted from tumor tissue and analyzed by Western blot for Vimentin expression. B-Actin antibody was used as the loading control. Densitometry of western blot of Vimentin/B-Actin. (B) Representative blots showing protein extracted from tumor tissue and analyzed by Western blot for TWIST1 expression. B-Actin antibody was used as the loading control. Densitometry of western blot TWIST1/B-Actin. (C) Representative blots showing protein extracted from tumor tissue and analyzed by Western blot for SLUG expression. B-Actin antibody used as loading control. Densitometry of western blot of SLUG/B-Actin. (D) Representative blots showing protein extracted from tumor tissue and analyzed by Western blot for E-cadherin expression. B-Actin antibody used as loading control. Densitometry of western blot of E-cadherin/B-Actin. Graphs represent mean per group (n=8–10 mice) and error bars are SEM. * $p<0.05$ between groups as indicated.

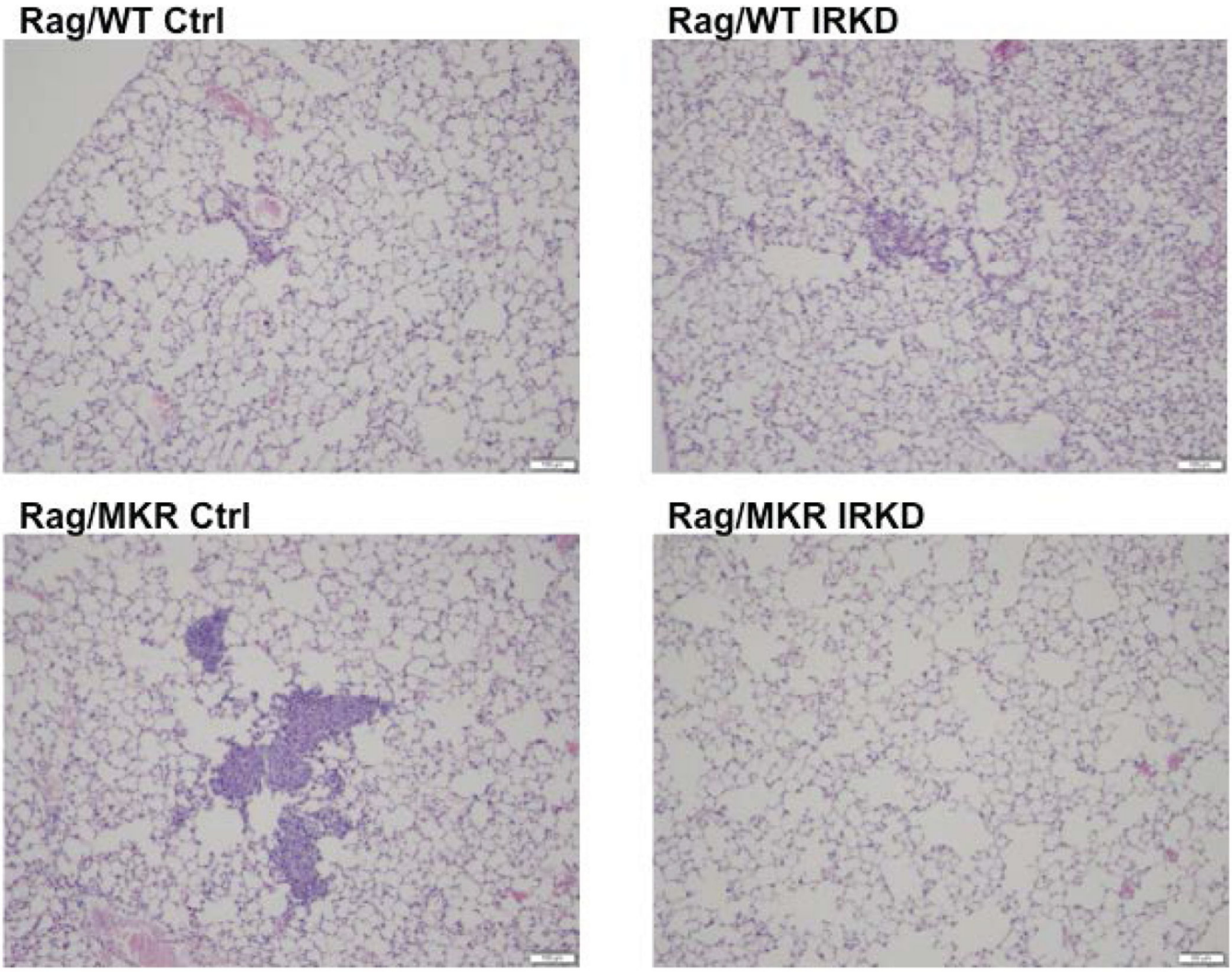

Figure 7.

Insulin Receptor Knockdown inhibited pulmonary metastases in hyperinsulinemic mice. Lungs were fixed, paraffin embedded and sectioned. Representative images of H&E stained lung sections from Rag/WT and Rag/MKR mice injected with LCC6 Ctrl and LCC6 IRKD cells. (A, B) 0/5 (0%) of Rag/WT injected with LCC6 Ctrl or LCC6 IRKD cells had pulmonary metastasis. (C) Representative pulmonary micrometastases seen in 2/5 (40%) Rag/MKR injected with LCC6 control cells. (D) 0/5 (0%) of Rag/MKR mice injected with LCC6 IRKD cells had pulmonary metastases. 10× magnification with scale bar of 100um in length.